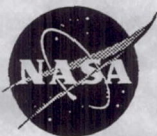6/27/94

R-8946

NASA Technical Memorandum 106642

Theoretical, Experimental, and Computational Evaluation of a Tunnel Ladder Slow-Wave Structure

Thomas M. Wallett and A. Haq Qureshi
Lewis Research Center
Cleveland, Ohio

June 1994

THEORETICAL, EXPERIMENTAL AND COMPUTATIONAL EVALUATION
OF A TUNNEL LADDER SLOW-WAVE STRUCTURE

Thomas Michael Wallett and A. Haq Qureshi*
National Aeronautics and Space Administration
Lewis Research Center
Cleveland, Ohio 44135

SUMMARY

The dispersion characteristics of a tunnel ladder circuit in a ridged wave guide were experimentally measured and determined by computer simulation using the electromagnetic code MAFIA. To qualitatively estimate interaction impedances, resonance frequency shifts due to a perturbing dielectric rod along the axis were also measured indicating the axial electric field strength. A theoretical modeling of the electric and magnetic fields in the tunnel area was also done.

INTRODUCTION

Of a variety of structures considered in recent years for possible applications at millimeter-wave frequencies, one that has received attention is the thin ladder circuit which was presented conceptually by Karp in 1955 [1] and its modification discussed by him in 1960 [2]. Similar parallel line and ladder structures were analyzed by Pierce [3] and Butcher [4] without space harmonics and by Froom et al. [5] and Kosmahl and O'Malley [6] using space harmonics. The predicted dispersion characteristics were in close agreement in all, however the values of interaction impedance varied. In their presentation, Kosmahl and O'Malley suggested that high beam operating voltages in the range of tens of kilovolts would make possible a non-space harmonic operation of a forward-wave ladder based amplifier at millimeter wavelengths. They also suggested that the gain rate would further benefit from the high interaction impedance associated with the ladder. Kosmahl and Palmer conducted an analysis of the idealized or modified Karp circuit referred to as the TunneLadder [7]. Their results pointed out to the suitability of this structure as a high impedance, narrow bandwidth circuit of about 1% that is voltage tunable over a frequency range of 5% and has excellent heat handling capability.
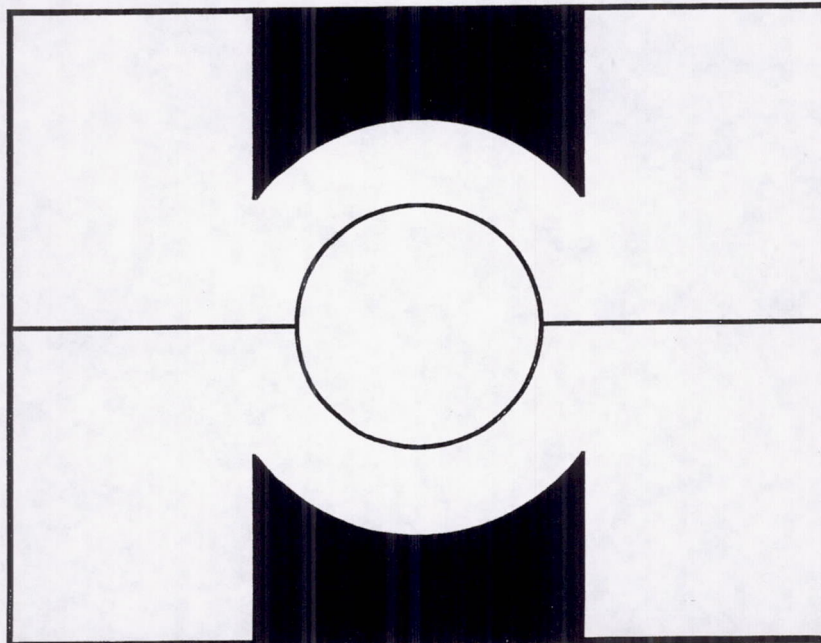

Figure 1 - Idealized circular tunnel ladder structure.

A simplified theoretical model of the TunneLadder structure was used by Kosmahl to predict the dispersion characteristics and interaction impedances (Figure 1). This model uses a circular wire loop to represent the hexagonal cross section of the actual tunnel region. The electric and magnetic fields are represented in cylindrical geometry inside the loop region and by Cartesian geometry outside the region. The boundary conditions are then applied at the various regions.

The actual TunneLadder is a novel, high impedance structure that was introduced by Karp and does not lend itself to a closed form analysis. The idealized structure, although quite simplified, is more amenable to closed form solution. With the idealized tunnel cross-sectional area equal to the actual cross-sectional area, the model predicts at least qualitatively the dispersion characteristics of both the symmetric and antisymmetric ladder modes.

A 29 GHz TWT utilizing the TunneLadder structure was fabricated and tested by Varian under a NASA contract [8,9]. The test results confirmed the potential applicability of the ladder-based structures for use in millimeter-wave traveling-wave tubes.

THEORETICAL EVALUATION OF THE ELLIPTICAL TUNNEL

A realistic approach would be to approximate the actual hexagonal tunnel cross section as an ellipse supported by dielectric slabs (Figure 2).
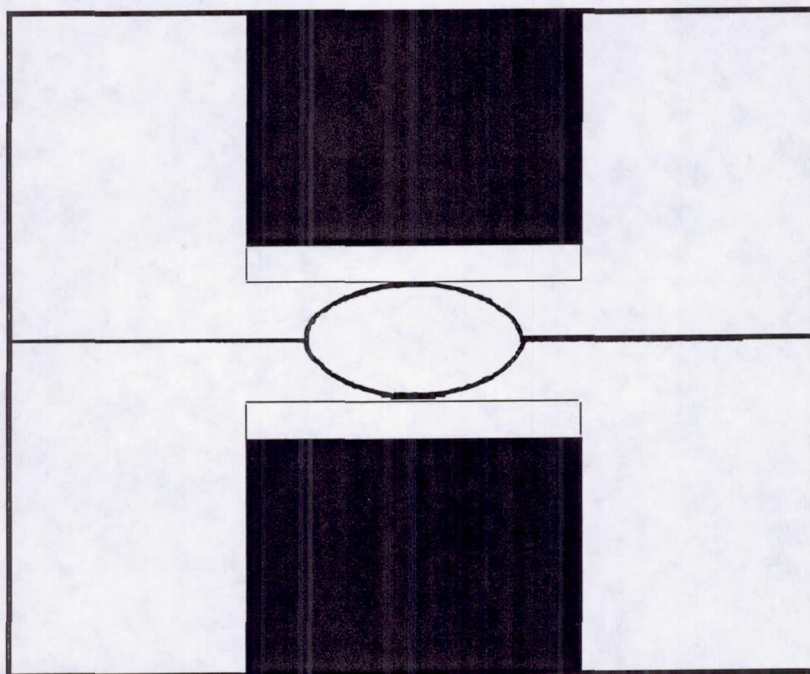

Figure 2 - Idealized elliptical tunnel ladder structure supported by dielectric slabs.

For this analytical effort, elliptic cylinder coordinates would be the preferred choice for field representation. The result would be a model to closely represent the electric and magnetic fields inside the tunnel region.

Electromagnetic waves propagating in elliptical metal pipes have been investigated as early as 1938 [10]. Since then several papers dealing with wave propagation [11], computation of critical frequencies [12] and cutoff wavelengths [13,14,15], and attenuation characteristics for elliptical [16,17] and dielectric-tube wave guides [18] have been published.

2

Cartesian coordinates in three dimensions are related to elliptic cylindrical coordinates by $x = d\,\cos(\vartheta)\,\cosh(\mu)$, $y = d\,\sin(\vartheta)\,\sinh(\mu)$, and $z = z$ where d is half the interfocal distance. The z-axis is chosen to be along the direction of propagation with the axial propagation constant designated as β. Propagating solutions in the z-direction are of the form $e^{-j\beta z}$. The remaining transverse Helmholtz equation $\nabla_T^2 \psi + k_T^2 \psi = 0$ where $k_T^2 = (\omega/c)^2 - \beta^2$ in the two-dimensional elliptic coordinate system is

$$\frac{\partial^2 \psi}{\partial \mu^2} + \frac{\partial^2 \psi}{\partial \vartheta^2} + d^2 k_T^2 [\cosh^2(\mu) - \cos^2(\vartheta)]\psi = 0. \tag{1}$$

Assuming $\psi = M(\mu)\,\Theta(\vartheta)$, the transverse Helmholtz equation separates into two equations with coupled eigenvalues, $h = k_T d$ and b:

$$\mathrm{d}^2 M/\mathrm{d}\mu^2 + [h^2 \cosh^2(\mu) - b]M = 0 \tag{2}$$

and

$$\mathrm{d}^2\Theta/\mathrm{d}\vartheta^2 + [b - h^2 \cos^2(\vartheta)]\Theta = 0. \tag{3}$$

Solutions for Θ are the Mathieu functions Se_m and So_m while the corresponding radial solutions for M are the modified Mathieu functions of the first kind, Je_m and Jo_m, and of the second kind, Ne_m and No_m, where m refers to the particular order of the function [19]. The functions $Se_m(h, \cos\vartheta)$ are even in ϑ with eigenvalues b designated as $be_m(h)$ while the functions $So_m(h, \cos\vartheta)$ are odd in ϑ with eigenvalues b designated as $bo_m(h)$. For a given h, the eigenvalues are ordered such that $be_0 < bo_1 < be_1 < \ldots < bo_m < be_m < bo_{m+1}\cdots$.

Inside the elliptical tunnel the continuity of ψ in value and slope at $\mu = 0$ prohibits corresponding radial solutions of the second kind, Ne_m and No_m. Therefore when the solution for Θ is $Se_m(h, \cos\vartheta)$ then the corresponding radial solution for M becomes $Je_m(h, \cosh\mu)$. Likewise, when the solution for Θ is $So_m(h, \cos\vartheta)$ then the corresponding radial solution for M becomes $Jo_m(h, \cosh\mu)$. Also on the metallic ellipse boundary at $\mu = \mu_0$, the z-component of the electric field must be zero.

There exist transverse magnetic (TM) and transverse electric (TE) modes in an elliptical wave guide not to mention hybrid modes. The modes are designated TM_{lmn} or TE_{lmn} where the index l is either c (standing for cosine or even) or s (standing for sine or odd). The m is an integer representative of the order, and n represents the nth parametric zero of the Mathieu function. For tube devices only the TM modes are useful. The field configuration for the lowest transverse magnetic (TM) mode in an elliptical wave guide is the TM_{c01} mode; the TM_{s01} does not exist [20]. The fields for this mode are well known and given in terms of the zero-order, even Mathieu functions and their derivatives.

$$E_\mu = \left(\frac{-j\beta_{c01}}{lk_{c\ c01}^2}\right) C_{01}\, Je_0'(h, \cosh\mu)\, Se_0(h, \cos\vartheta)\, \exp\{j(\omega t - \beta_{c01} z)\} \tag{4}$$

$$E_\vartheta = \left(\frac{-j\beta_{c01}}{lk_{c\ c01}^2}\right) C_{01}\, Je_0(h, \cosh\mu)\, Se_0'(h, \cos\vartheta)\, \exp\{j(\omega t - \beta_{c01} z)\} \tag{5}$$

$$E_z = C_{01}\, Je_0(h, \cosh\mu)\, Se_0(h, \cos\vartheta)\, \exp\{j(\omega t - \beta_{c01} z)\} \tag{6}$$

$$H_\mu = \left(\frac{j\omega\epsilon_0}{lk_{c\ c01}^2}\right) C_{01}\, Je_0(h, \cosh\mu)\, Se_0'(h, \cos\vartheta)\, \exp\{j(\omega t - \beta_{c01} z)\} \tag{7}$$

$$H_\vartheta = \left(\frac{-j\omega\epsilon_0}{lk_{c\ c01}^2}\right) C_{01}\, Je_0'(h, \cosh\mu)\, Se_0(h, \cos\vartheta)\, \exp\{j(\omega t - \beta_{c01} z)\} \tag{8}$$

$$H_z = 0 \tag{9}$$

Here $l = d\sqrt{\dfrac{\cosh(2\mu) - \cos(2\vartheta)}{2}}$, $k_{c\ c01}$ is the transverse cutoff wave number, the cutoff axial

propagation constant is $\beta_{c\ c01} = \sqrt{(\omega^2/c^2) - k_{c\ c01}^2}$, and C_{01} is a normalization coefficient.

The power flow through the tunnel region can be found from

$$P = \frac{1}{2} \int\limits_0^{\mu_0} \int\limits_0^{2\pi} (E_\mu H_\vartheta^* - E_\vartheta H_\mu^*) l^2 \ d\vartheta \ d\mu. \tag{10}$$

To completely specify the fields for the TM_{c01} mode, the transverse cutoff wave number $k_{c\ c01}$ must be found. Since this is related to the eigenvalue h, we must determine h such that E_z is zero at the ellipse boundary $\mu = \mu_0$.

Since the eigenvalues h and b depend on each other, they must be found simultaneously. Solution of the eigenvalues h and b involves the evaluation of continued fractions [21]. For m an integer, the eigenvalues are related through

$$b = m^2 + \frac{h^2}{4}\left[2 + \frac{a_1}{a_0} + \frac{a_{-1}}{a_0}\right] \tag{11}$$

where the a coefficients are to be determined. The ratios a_1/a_0 and a_{-1}/a_0 are given by the continued fractions

$$\frac{a_n}{a_{n-1}} = \frac{-h^2}{16(m/2 + n)^2 + 2h^2 - 4b + h^2(a_{n+1}/a_n)} \tag{12}$$

and

$$\frac{a_n}{a_{n+1}} = \frac{-h^2}{16(m/2 + n)^2 + 2h^2 - 4b + h^2(a_{n-1}/a_n)}. \tag{13}$$

For the lowest order mode, $m = 0$, the ratio $a_1/a_0 = a_{-1}/a_0$.

For large positive n, $\dfrac{a_{n+1}}{a_n} \approx \dfrac{-h^2}{16(m/2 + n)^2}$ and for large negative n, $\dfrac{a_{n-1}}{a_n} \approx \dfrac{-h^2}{16(m/2 + n)^2}$.

Substituting these limiting values in equations (12) and (13), the ratios a_1/a_0 and a_{-1}/a_0 are found and the eigenvalue relation in continued fraction form becomes

$$2b = h^2 - \cfrac{h^4}{16(1)^2 + 2h^2 - 4b - \cfrac{h^4}{16(2)^2 + 2h^2 - 4b - \cfrac{h^4}{16(3)^2 + 2h^2 - 4b - \ldots}}}. \tag{14}$$

The condition that $E_z = 0$ at $\mu = \mu_0$ is now needed to finally solve for both h and b. This is equivalent to finding h which satisfies

$$Je_0(h, \cosh \mu_0) = 0. \tag{15}$$

The Mathieu function $Je_0(h, \cosh \mu_0)$ can be calculated as a summation of Bessel functions

$$Je_0(h, \cosh \mu_0) = \sqrt{\pi/2} \sum_{n=0}^{\infty} (-1)^n B_{2n} J_{2n}(h \cosh \mu_0) \tag{16}$$

where

$$B_{2n} = \frac{a_n}{\left[\displaystyle\sum_{n=0}^{\infty} a_n\right]}. \tag{17}$$

4

The procedure then to solve for the proper eigenvalues, given the particular tunnel dimensions, is to pick a value for h and solve for b using equation (14). Using h and b one can find the coefficients a_n to determine the B_{2n} coefficients. After solving equation (15) for h using equation (16), the procedure is repeated. Once the eigenvalues h and b are found then values for $k_{c\ c01}$ and $\beta_{c\ c01}$ are calculated. With this the unnormalized fields for the elliptical tunnel region are determined from equation (4) through (9).

A BASIC program has been written to calculate the eigenvalue b for a particular eigenvalue h. The actual solution of both eigenvalues simultaneously given a set of tunnel dimensions was achieved using the program MATHCAD. To determine the dispersion characteristics of the tunnel ladder structure the fields exterior to the tunnel region must be found and only by matching admittances at the elliptical boundary can a closed form dispersion relation be realized. Since the region exterior lends itself to Cartesian coordinates, only a crude match can be achieved. A relatively simple closed form solution of such a complicated problem is not warranted since results can only be qualitative in nature. However, if the power and dispersion characteristics of the particular tunnel ladder can be found by other means, the use of the E_z field for calculation of interaction impedance may prove useful.

EXPERIMENTAL EVALUATION

For the experimental determination of the dispersion characteristics a 29 GHz tunnel ladder structure similar to the Varian structure has been fabricated (Figure 3).
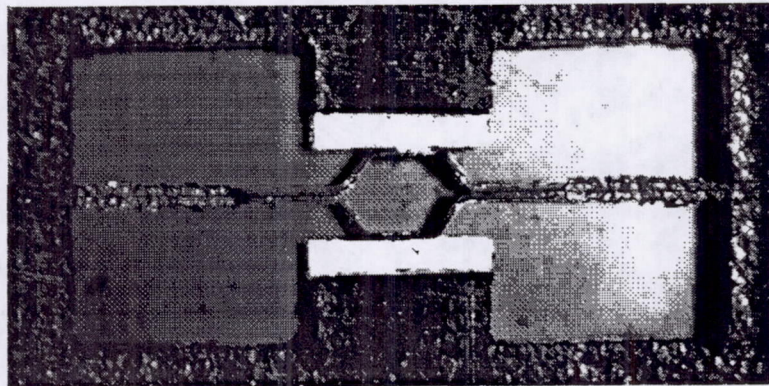

Figure 3 - Cross-section of the experimental tunnel ladder structure.

In fact, two copper ladders manufactured by Varian for contract number NAS3-23347 each having a slight depression in the middle of the rungs were placed together to form the tunnel ladder. The tunnel was hexagonal in shape with a width of 0.0386 inch and a height of 0.0252 inch. Ladder and structure dimensions were measured using an optical microscope. Each ladder consisted of 101 rungs and was 0.0025 inch thick with 0.0066 inch wide rungs and 0.006 inch wide by 0.1105 inch long slot spaces.

A ridged wave guide was fabricated using electrical discharge machining (EDM) from copper block in two symmetrical halves. The width and height of the entire cavity of the ridged wave guide were 0.212 inch and 0.098 inch, respectively. The cross-section dimension of the ridges was approximately 0.0575 inch wide by 0.0214 inch high. Two amorphous boron nitride ($\epsilon_r = 3.973$) dielectric slabs, 0.0575 inch wide by 0.0125 inch high and glued to both the upper and lower ridges, were used to support both ladders. The ladders were positioned between the two halves of the ridged wave guide such that the rungs on both ladders were aligned. Screws were used to finally secure both halves of the ridged wave guide. A 17-period length of the test structure was cut using wire EDM. Minor dimensional inconsistencies in the structure are apparent and are due to the specific machining processes and fabrication methods.

5

Since the anticipated high frequency cutoff was near 30 GHz, the tunnel ladder structure was initially tested using an HP 8510C network analyzer in WR-28 wave guide. The signal was coupled through small holes drilled into the wide faces of the input and output wave guides at the ends of the tunnel ladder structure. The attenuation of the signal through the coupling holes was too great, however, and no resonances were observed. Any attempt to enlarge the holes would diminish the shorting effect at the ends of the structure.

It was decided to use another HP 8510C network analyzer which can operate in coaxial cable up to 40 GHz. A test fixture was machined out of brass in which K-connectors were installed in both halves such that the signal coupling was achieved from coaxial probes through small holes drilled in each half of the fixture. Grooves to fit the length and width of the entire structure were milled on the insides of each half of the fixture to center the tunnel horizontally and vertically with the probes. An alignment pin connected both halves (Figure 4).
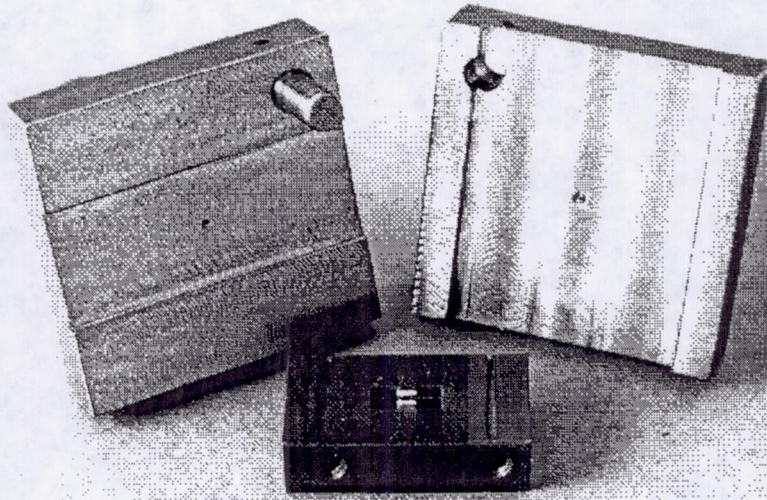

Figure 4 - **Experimental tunnel ladder structure and test fixture.**

The assembled 17-period tunnel ladder structure and test fixture were connected to the network analyzer using 2.4 mm coaxial cable (Figure 5).
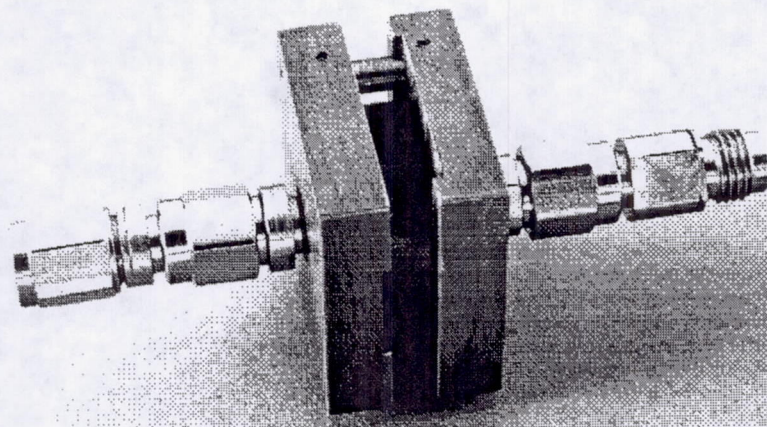

Figure 5 - **Assembled experimental tunnel ladder structure and test fixture.**

Measurements from 10 GHz to 35 GHz of the resonance frequencies for the structure were taken with (Figure 6) and without (Figure 7) an alumina rod ground to a 0.025 inch diameter and inserted in the tunnel region.

Six resonances were observed for both sets of measurements. The K-connectors will exhibit a resonance just above 30 GHz, but this offered no problem since transmission through the structure was negligible near this frequency.

S21   lin MAG
REF -100.0 mUnits
     50.0 mUnits

START   10.000000000 GHz
STOP   35.000000000 GHz
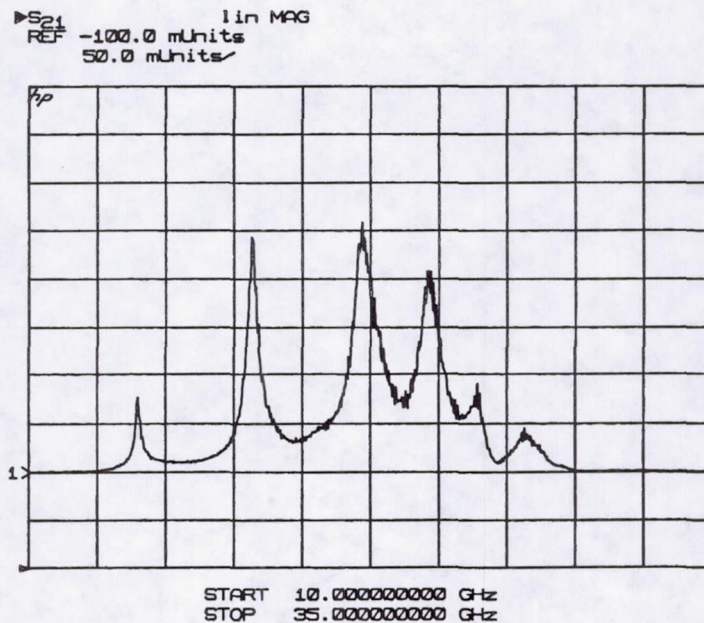
Figure 6 - Transmission measurement of the tunnel ladder structure without the dielectric rod.

S21   lin MAG
REF -200.0 mUnits
     100.0 mUnits

START   10.000000000 GHz
STOP   35.000000000 GHz

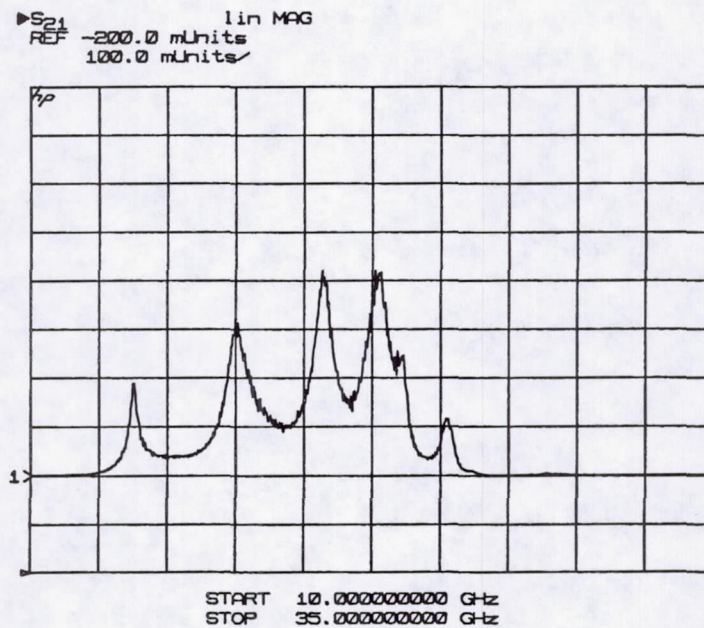**Figure 7** - Transmission measurement of the tunnel ladder structure with the dielectric rod.

7

COMPUTATIONAL EVALUATION

The tunnel ladder structure was also modeled using the MAFIA code. The MAFIA code allows the generation of elliptical cylinders very easily. One period of the actual hexagonal tunnel ladder was therefore modeled as an elliptical tunnel ladder, having the same cross-sectional area with the same ladder thickness. The height and width of the hexagonal tunnel were used to find the eccentricity e of the ellipse with semimajor axis r_a and semiminor axis r_b.

$$\frac{\sqrt{(width)^2 - (height)^2}}{height} = e = \frac{\sqrt{r_a^2 - r_b^2}}{r_a} \tag{18}$$

The semimajor and semiminor axes were then found simultaneously from the tunnel area using

$$\pi r_a r_b = Area \tag{19}$$

The dimensions of the simulated ridged wave guide and dielectric supports were chosen as close to the actual dimensions as possible such that bilateral symmetry was preserved vertically and horizontally with respect to the center of the tunnel.

A simulated dielectric rod was given the same dimensions as the actual alumina rod and was located in the elliptical tunnel. The shape of the simulated rod cross-section is not quite circular. This is due to the resolution of the mesh. A finer resolution would improve the shape, however the computer time involved would dramatically increase. The mesh for one period of the structure was chosen to be a uniform 85 x 40 x 5 (Figure 8).
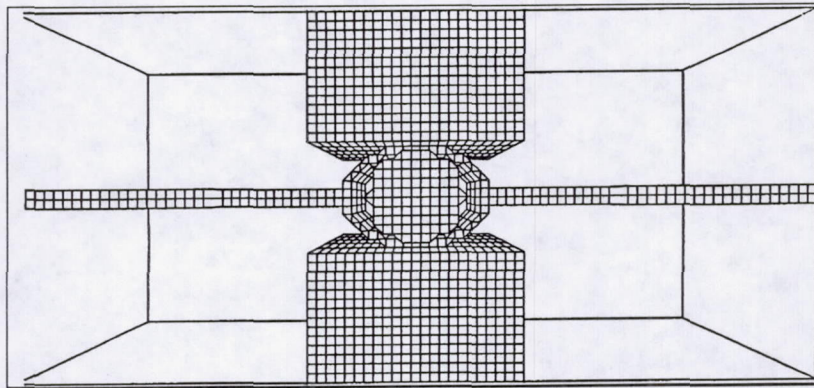

Figure 8 - MAFIA computer mesh simulation of the tunnel ladder structure.

Computer runs to generate the mesh, set up the eigenvalue matrix, and solve for the eigenvalues (frequency resonances) for the two cases, with and without the dielectric rod, were completed. In each case for each run the phase shift per period was adjusted from $(1/17) \cdot 180°$ to $(6/17) \cdot 180°$ to coincide with the experimentally measured frequency resonances.

COMPARISON OF RESULTS

Frequency resonance values generated by the MAFIA code were close to experimentally measured results. The simulated tunnel ladder structure was then modified to reflect the dimensional inconsistencies that were present in the actual structure. The code was run again and frequency values were even closer to the experimental results (Figure 9).
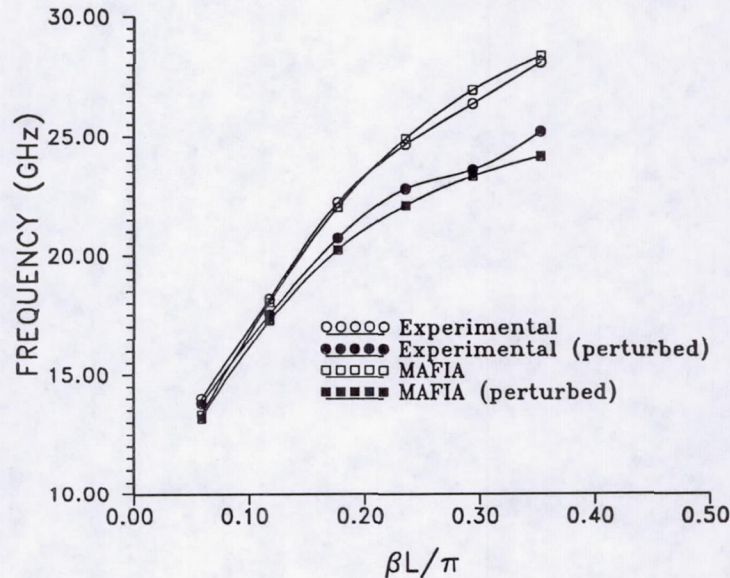
8

Figure 9 - Experimental and computer-generated tunnel ladder dispersion characteristics.

The frequency shifts for both the experimentally measured resonances and the computer-generated resonances also were very close and increased with frequency. This is indicative of a structure with good interaction impedance for a device where a nominal electron beam voltage may be used. The resonance frequencies and shifts in frequencies found using the MAFIA code were slightly greater in value than the experimental results. Any discrepancies in results can be attributed to the deviation of the actual structure dimensions from the computer model, the computer mesh resolution, the dielectric constants for boron nitride and alumina, and the variation in the dielectric cross sections along the length of the structure. A much finer resolution would give a better description of the actual structure but this is really not needed considering the closeness of the results. Taking into account the actual variation and non-uniformity of the experimental tunnel ladder structure dimensions demonstrated the feasibility of the MAFIA code for use in the design of these structures.

CONCLUDING REMARKS

The ability to perform successful measurements on the actual tunnel ladder structure at the operating frequency is a major contribution towards the characterization and analysis of these particular slow-wave structures. Previously, scaled versions of the structure were constructed for cold testing to determine their suitability to operate successfully at higher frequencies. Also with the confidence gained with respect to the computer-generated dispersion characteristics, the ability to predict structure characteristics without the need to first fabricate the structure was demonstrated. It is much easier, faster, more versatile, and eventually cost effective to model the structure using computer-aided design software codes than to fabricate, test, and evaluate a prospective structure experimentally to initially determine its potential. Furthermore, variations in the geometry of the structure to achieve the desired characteristics can be incorporated easily and therefore highly efficient structures can be designed without prohibitive costs of trial fabrication and testing.

It remains for future work to expand the theoretical model of the tunnel ladder structure or develop other models to predict with accuracy the dispersion characteristics. Improved fabrication methods to reduce structure losses are definitely needed. Although the exact theoretical description of many novel structures is extremely difficult, preliminary investigations should be conducted to at least approximately characterize the structure in question.

With the recent availability of reliable electromagnetic computer programs capable of solving Maxwell's equations in three dimension, a wide variety of periodic slow-wave structures can be designed and evaluated easily and without exorbitant cost. The various types of structures that can be investigated are limited solely to the imagination of the designer.

ACKNOWLEDGEMENT

APPENDIX A

Mathcad program to find the Mathieu function eigenvalues h and b for the elliptical tunnel region.

Read frequency data file $M := \text{READPRN}(\text{tlexp})$ **speed of light** $c := 2.99792 \cdot 10^8$

frequencies $f := M^{<0>} \cdot 10^9$ $\omega := 2 \cdot \pi \cdot f$ **permittivity** $\varepsilon := 8.854 \cdot 10^{-12}$

number of points $N := \text{length}(f)$ $N = 6$ **period** $L := .0126 \cdot .0254$

axial wavenumbers $i := 1 .. N$ $\beta_i := \dfrac{\pi}{L} \cdot \dfrac{i}{17}$ **17 periods of the structure**

Define elliptical parameters.

semimajor axis $\text{semimajor} := .0386 \cdot .0127$ **semiminor axis** $\text{semiminor} := .0252 \cdot .0127$

Calculate the radial elliptical coordinate for the ellipse.

$$\mu1 := \frac{1}{2} \cdot \ln\left(\frac{\text{semimajor} + \text{semiminor}}{\text{semimajor} - \text{semiminor}}\right) \qquad \mu1 = 0.78025$$

Calculate the eccentricity of the ellipse.

$$\text{ecc} := \frac{\sqrt{\text{semimajor}^2 - \text{semiminor}^2}}{\text{semimajor}} \qquad \text{ecc} = 0.75749$$

Calculate the interfocal distance.

$d := \text{semimajor} \cdot \text{ecc}$ $d = 3.71335 \cdot 10^{-4}$

Find the eigenvalues h and b using continued fractions for the TM_{c01} mode.

$\text{limit} := 10$ $m := 0$ $se := 2 \cdot m$ $so := 2 \cdot m + 1$

$n := \text{limit} .. 1$ $s := se$ $h := 1.9818$ $b := 1.52368$

$$\text{pratio}_{\text{limit}+1} := \frac{-h^2}{16 \cdot \left(\text{limit} + \frac{1}{2} \cdot s\right)^2} \qquad\qquad \text{pratio}_n := -\frac{h^2}{16 \cdot \left(\frac{1}{2} \cdot s + n\right)^2 + 2 \cdot h^2 - 4 \cdot b + h^2 \cdot \text{pratio}_{n+1}}$$

$$\text{nratio}_{\text{limit}+1} := \frac{-h^2}{16 \cdot \left(\frac{1}{2} \cdot s - \text{limit}\right)^2} \qquad\qquad \text{nratio}_n := -\frac{h^2}{16 \cdot \left(\frac{1}{2} \cdot s - n\right)^2 + 2 \cdot h^2 - 4 \cdot b + h^2 \cdot \text{nratio}_{n+1}}$$

Given $s^2 = b - \dfrac{h^2}{4} \cdot \left(2 + \text{pratio}_1 + \text{nratio}_1\right)$ $b := \text{find}(b)$ $b = 1.52368$

Calculate the B_{2n} coefficients.

$n := 0 .. \text{limit}$ $a_0 := 1$ $a_{n+1} := \text{pratio}_{n+1} \cdot a_n$ $B_{2 \cdot n} := \dfrac{a_n}{\sum\limits_n a_n}$ $\sum\limits_n B_{2 \cdot n} = 1$

11

Even solutions of period π
s = even integer = $2m$, allowed values of b = be_{2m}

$$See(\phi) := \sum_n B_{2 \cdot n} \cdot \cos(2 \cdot n \cdot \phi)$$

$$Jee(h,\mu) := \sqrt{\frac{\pi}{2}} \cdot \sum_n \left[(-1)^{n-m} \cdot B_{2 \cdot n} \cdot Jn(2 \cdot n, h \cdot \cosh(\mu)) \right]$$

$$Nee(h,\mu) := \sqrt{\frac{\pi}{2}} \cdot \sum_n \left[(-1)^{n-m} \cdot B_{2 \cdot n} \cdot Yn(2 \cdot n, h \cdot \cosh(\mu)) \right]$$

Even solutions of period 2π
s = odd integer = $2m + 1$, allowed values of b = be_{2m+1}

$$Seo(\phi) := \sum_n B_{2 \cdot n+1} \cdot \cos((2 \cdot n + 1) \cdot \phi)$$

$$Jeo(h,\mu) := \sqrt{\frac{\pi}{2}} \cdot \sum_n (-1)^{n-m} \cdot B_{2 \cdot n+1} \cdot Jn(2 \cdot n + 1, h \cdot \cosh(\mu))$$

$$Neo(h,\mu) := \sqrt{\frac{\pi}{2}} \cdot \sum_n (-1)^{n-m} \cdot B_{2 \cdot n+1} \cdot Yn(2 \cdot n + 1, h \cdot \cosh(\mu))$$

Odd solutions of period π
s = even integer = $2m$, allowed values of b = be_{2m}

$$Soe(\phi) := \sum_n B_{2 \cdot n} \cdot \sin(2 \cdot n \cdot \phi)$$

$$Joe(h,\mu) := \sqrt{\frac{\pi}{2}} \cdot \tanh(\mu) \cdot \sum_n (-1)^{n-m} \cdot (2 \cdot n) \cdot B_{2 \cdot n} \cdot Jn(2 \cdot n, h \cdot \cosh(\mu))$$

$$Noe(h,\mu) := \sqrt{\frac{\pi}{2}} \cdot \tanh(\mu) \cdot \sum_n (-1)^{n-m} \cdot (2 \cdot n) \cdot B_{2 \cdot n} \cdot Yn(2 \cdot n, h \cdot \cosh(\mu))$$

Odd solutions of period 2π
s = odd integer = $2m + 1$, allowed values of b = be_{2m+1}

$$Soo(\phi) := \sum_n B_{2 \cdot n+1} \cdot \sin((2 \cdot n + 1) \cdot \phi)$$

$$Joo(h,\mu) := \sqrt{\frac{\pi}{2}} \cdot \tanh(\mu) \cdot \sum_n (-1)^{n-m} \cdot (2 \cdot n + 1) \cdot B_{2 \cdot n+1} \cdot Jn(2 \cdot n + 1, h \cdot \cosh(\mu))$$

$$Noo(h,\mu) := \sqrt{\frac{\pi}{2}} \cdot \tanh(\mu) \cdot \sum_n (-1)^{n-m} \cdot (2 \cdot n + 1) \cdot B_{2 \cdot n+1} \cdot Yn(2 \cdot n + 1, h \cdot \cosh(\mu))$$

Condition for E_z to be zero on the ellipse.

Given $Jee(h, \mu 1) = 0$ $h := find(h)$ $h = 1.9818$ $b = 1.52368$

$$l(\mu, \phi) := d \cdot \sqrt{\cosh(\mu)^2 - \cos(\phi)^2} \qquad k1 := \frac{h}{d} \qquad kc_i := \sqrt{\left(\frac{\omega_{i-1}}{c}\right)^2 - \left(\beta_i\right)^2}$$

Field equations for the TM_{c01} mode.

$$E_z(\mu, \phi) := Jee(h, \mu) \cdot See(\phi) \qquad\qquad H_z := 0$$

$$E_\mu(i, \mu, \phi) := \beta_i \cdot \frac{d}{d\mu} Jee(h, \mu) \cdot See(\phi) \qquad H_\mu(i, \mu, \phi) := \omega_{i-1} \cdot \varepsilon \cdot Jee(h, \mu) \cdot \frac{d}{d\phi} See(\phi)$$

$$E_\phi(i, \mu, \phi) := \beta_i \cdot Jee(h, \mu) \cdot \frac{d}{d\phi} See(\phi) \qquad H_\phi(i, \mu, \phi) := \omega_{i-1} \cdot \varepsilon \cdot \frac{d}{d\mu} Jee(h, \mu) \cdot See(\phi)$$

Power flow through the elliptical cross section.

$$P_i := \frac{1}{2} \cdot \frac{1}{\left(kc_i\right)^4} \cdot \int_0^{\mu 1} \int_0^{2\cdot\pi} \left(E_\mu(i, \mu, \phi) \cdot H_\phi(i, \mu, \phi) + E_\phi(i, \mu, \phi) \cdot H_\mu(i, \mu, \phi) \right) d\phi \, d\mu$$

Interaction impedance

dielectric rod radius $r := .0125 \cdot .0254$

effective rod semimajor axis $a_r := \dfrac{r}{\sqrt{\sqrt{1 - ecc^2}}}$ **effective rod semiminor axis** $b_r := r \cdot \sqrt{\sqrt{1 - ecc^2}}$
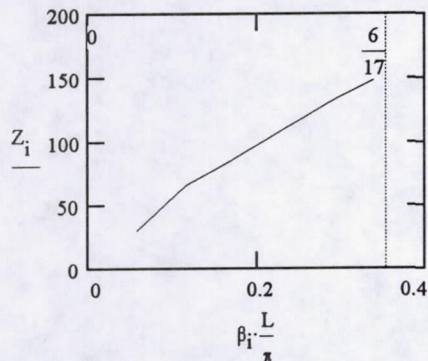
$a_r = 3.9295 \cdot 10^{-4}$

$b_r = 2.56537 \cdot 10^{-4}$

rod elliptic coordinate $\mu_r := \dfrac{1}{2} \cdot \ln\left(\dfrac{a_r + b_r}{a_r - b_r}\right)$ **interaction impedance** $Z_i := \dfrac{\displaystyle\int_0^{\mu_r} \int_0^{2\cdot\pi} E_z(\mu, \phi)^2 \cdot l(\mu, \phi)^2 \, d\phi \, d\mu}{2 \cdot \left(\beta_i\right)^2 \cdot P_i \cdot \pi \cdot r^2}$

$\mu_r = 0.78025$

Plot of interaction impedance based on power flow through the elliptic tunnel region only.

i	$f_{i-1} \cdot 10^{-9}$	Z_i
1	14	29.76528
2	18.1875	66.12221
3	22.21875	88.01017
4	24.65625	110.86925
5	26.375	133.2358
6	28.09375	152.53418

13

BASIC program to solve for the Mathieu function eigenvalue b given eigenvalue h and order s.

```
10  DIM PRATIO(15),NRATIO(15),DPRATIO(15),DNRATIO(15),APLUS(15),AMINUS(15),
      BPLUS(15),BMINUS(15)
20  CLS:INPUT "What is the order s";S:INPUT "What is h";H:INPUT "What is the guess for b";B
30  INPUT "What is the number coefficients required";N
40  REM-Figure a(n)/a(n-1)-------------------------------------------------------
50  PRATIO(N+1)=-H*H/16/(S/2+N)/(S/2+N)
60  FOR I=N TO 1 STEP -1
70     PRATIO(I)=-H*H/(16*(S/2+I)*(S/2+I)+2*H*H-4*B+H*H*PRATIO(I+1))
80  NEXT I
90  APLUS(0)=1:POSASUM=APLUS(0):POSBSUM=0
100 FOR I=1 TO N
110    APLUS(I)=PRATIO(I)*APLUS(I-1)
120    POSASUM=POSASUM+APLUS(I)
130 NEXT I
140 FOR I=0 TO N
150    BPLUS(I)=APLUS(I)/POSASUM
160    POSBSUM=POSBSUM+BPLUS(I)
170 NEXT I
180 REM-Figure a(-n)/a(-n+1)-----------------------------------------------------
190 NRATIO(N+1)=-H*H/16/(S/2-N)/(S/2-N)
200 FOR I=N TO 1 STEP -1
210    NRATIO(I)=-H*H/(16*(S/2-I)*(S/2-I)+2*H*H-4*B+H*H*NRATIO(I+1))
220 NEXT I
230 AMINUS(0)=1:NEGASUM=AMINUS(0):NEGBSUM=0
240 FOR I=1 TO N
250    AMINUS(I)=NRATIO(I)*AMINUS(I-1)
260    NEGASUM=NEGASUM+AMINUS(I)
270 NEXT I
280 FOR I=0 TO N
290    BMINUS(I)=AMINUS(I)/NEGASUM
300    NEGBSUM=NEGBSUM+BMINUS(I)
310 NEXT I
320 REM-Finding b-----------------------------------------------------------------
330 DPRATIO(N+1)=0
340 FOR I=N TO 1 STEP -1
350    DPRATIO(I)=PRATIO(I)*
         (4-H*H*DPRATIO(I+1))/(16*(S/2+I)*(S/2+I)+2*H*H-4*B+H*H*DPRATIO(I+1))
360 NEXT I
370 F=B-H*H/4*(2+PRATIO(1)+NRATIO(1))-S*S
380 DF=1-H*H/4*(DPRATIO(1)+DNRATIO(1))
390 BNEW=B-F/DF:IF ABS(BNEW-B)>.00001 THEN B=BNEW/2+B/2:
      PRINT "b=";B:GOTO 40
400 PRINT "N","a+=","B+=","a-=","B-="
410 FOR I=0 TO N
420    PRINT I,APLUS(I),BPLUS(I),AMINUS(I),BMINUS(I)
430 NEXT I
440 PRINT "h=";H,"b=";B
450 PRINT "positive a sum=";POSASUM,"negative a sum=";NEGASUM
460 PRINT "positive b sum=";POSBSUM,"negative b sum=";NEGBSUM
470 END
```

APPENDIX C

Mathieu Eigenfunction Solutions: Periodic in ϑ, suitable for ϑ real.

Even solutions about $\vartheta = 0$; $b = be_{2m}$ or be_{2m+1}.

$$Se_{2m}(h, \cos \vartheta) = \sum_{n=0}^{\infty} B_{2n} \cos(2n\vartheta); \quad \sum_{n} B_{2n} = 1$$

$$Se_{2m+1}(h, \cos \vartheta) = \sum_{n=0}^{\infty} B_{2n+1} \cos[(2n+1)\vartheta]; \quad \sum_{n} B_{2n+1} = 1$$

Odd solutions about $\vartheta = 0$; $b = bo_{2m}$ or bo_{2m+1}.

$$So_{2m}(h, \cos \vartheta) = \sum_{n=1}^{\infty} B_{2n} \sin(2n\vartheta); \quad \sum_{n}(2n) B_{2n} = 1$$

$$So_{2m+1}(h, \cos \vartheta) = \sum_{n=0}^{\infty} B_{2n+1} \sin[(2n+1)\vartheta]; \quad \sum_{n}(2n+1) B_{2n+1} = 1$$

Corresponding Radial Solutions

For $\mu = i\vartheta$ and for values of the B's and of b corresponding to the angular functions Se, So.

Even functions:

$$Je_{2m}(h, \cosh \mu) = \sqrt{\pi/2} \sum_{n=0}^{\infty} (-1)^{n-m} B_{2n} J_{2n}(h \cosh \mu)$$

$$Je_{2m+1}(h, \cosh \mu) = \sqrt{\pi/2} \sum_{n=0}^{\infty} (-1)^{n-m} B_{2n+1} J_{2n+1}(h \cosh \mu)$$

Odd functions:

$$Jo_{2m}(h, \cosh \mu) = \sqrt{\pi/2} \tanh \mu \sum_{n=1}^{\infty} (-1)^{n-m}(2n) B_{2n} J_{2n}(h \cosh \mu)$$

$$Jo_{2m+1}(h, \cosh \mu) = \sqrt{\pi/2} \tanh \mu \sum_{n=0}^{\infty} (-1)^{n-m}(2n+1) B_{2n+1} J_{2n+1}(h \cosh \mu)$$

REFERENCES

[1]   A. Karp, "Traveling wave tube experiments at millimeter wavelengths with a new, easily built, space-harmonic circuit," *Proc. IRE*, vol. 43, pp. 41-46, (1955).

[2]   A. Karp, "Millimetre-wave valves," in Fortschritte der Hochfrequenztechnik, M. Strutt *et al.*, eds, vol. 5, pp. 73-128, Academic Press MBH, Frankfurt/Main, 1960.

[3]   J. R. Pierce, "Propagation in linear arrays of parallel wires," *IRE Trans. Electron Devices*, vol. ED-2, pp. 13-24, Jan., 1955.

[4]   P. N. Butcher, "A theoretical study of propagation along tape ladder lines and the coupling impedance of tape structures," *Proc. IEE*, vol. B104, pp. 169-187, Mar., 1957.

[5]   J. Froom, A. Pearson, E. A. Ash, and A. W. Horsley, "Ridge-loaded ladder lines," *IEEE Trans. Electron Devices*, vol. ED-12, pp. 411-421, Jul., 1965.

[6]   H. G. Kosmahl and T. A. O'Malley, "Harmonic analysis of the forward wave Karp structure," presented at 1978 Microwave Power Tube Conf. (Monterey, CA, Apr. 30, 1978).

[7]   H. G. Kosmahl and R. W. Palmer, "Harmonic analysis approach to the 'TunneLadder': A modified Karp circuit for millimeter-wave TWTA's," *IEEE Trans. Electron Devices*, vol. ED-29, no. 5, pp. 862-869, May, 1982.

[8]   A. Jacquez, A. Karp, D. Wilson, and A. Scott, "A millimeter-wave TunneLadder TWT," NASA contractor report 182184, Varian Associates, Inc., Aug., 1988.

[9]   D. Wilson, "A millimeter-wave tunneladder TWT," NASA contract report 182183, Varian Associates, Inc., Oct., 1988.

[10]   L. J. Chu, "Electromagnetic wave in elliptic hollow pipes of metal," *Journal of Applied Physics*, vol. 9, pp. 583-591, Sep., 1938.

[11]   J. G. Kretzschmar, "Wave propagation in hollow conducting elliptical waveguides," *IEEE Transactions on Microwave Theory and Techniques*, vol. MTT-18, no. 9, pp. 547-554, Sep., 1970.

[12]   S. B. Rayevskiy and V. YA. Smorgonskiy, "Method of computation of critical frequencies of an elliptical waveguide," *Radio Engineering and Electron Physics*, vol. 15, no. 9, pp. 1702-1705, Sep. 17, 1969.

[13]   A. A. El-Sherbiny, "Cutoff wavelengths of ridged, circular, and elliptic guides," *IEEE Transactions on Microwave Theory and Techniques*, vol. MTT-21, no. 1, pp. 7-12, Jan., 1973.

[14]   J. B. Davies *et al.*, "Analysis of hollow elliptical waveguides by polygon approximation," *Proc. IEE*, vol. 119, no. 5, pp. 519-522, May, 1972.

[15]   J. Mazumdar, "A method for the study of TE and TM modes in waveguides of very general cross section," *IEEE Transactions on Microwave Theory and Techniques*, vol. MTT-28, no. 9, pp. 991-995, Sep., 1980.

[16]   J. G. Kretzschmar, "Attenuation characteristics of hollow conducting elliptical waveguides," *IEEE Transactions on Microwave Theory and Techniques*, vol. MTT-20, no. 4, pp. 280-284, Apr., 1972.

[17]   L. Lewin and A. M. B. Al-Hariri, "The effect of cross-section curvature on attenuation in elliptic waveguides and a basic correction to previous formulas," *IEEE Transactions on Microwave Theory and Techniques*, vol. MTT-22, no. 5, pp. 504-509, May, 1974.

[18]   S. R. Rengarajan *et al.*, "Propagation characteristics of elliptical dielectric-tube waveguides," *IEE Proc.*, vol. 127, Pt. H, no. 3, pp. 121-126, Jun., 1980.

[19]   P. M. Morse and H. Feshbach, "Methods of Theoretical Physics," Part II, pp. 1407-1412, McGraw-Hill Book Company, New York, NY, 1953.

[20]   J. G. Kretzschmar, "Field configuration of the TM_{01} mode in an elliptical waveguide," *Proc. IEE*, vol. 118, no. 9, pp. 1187-1189, Sep., 1971.

[21]   P. M. Morse and H. Feshbach, "Methods of Theoretical Physics," Part I, pp. 562-567, McGraw-Hill Book Company, New York, NY, 1953.

REPORT DOCUMENTATION PAGE

Public reporting burden for this collection of information is estimated to average 1 hour per response, including the time for reviewing instructions, searching existing data sources, gathering and maintaining the data needed, and completing and reviewing the collection of information. Send comments regarding this burden estimate or any other aspect of this collection of information, including suggestions for reducing this burden, to Washington Headquarters Services, Directorate for Information Operations and Reports, 1215 Jefferson Davis Highway, Suite 1204, Arlington, VA 22202-4302, and to the Office of Management and Budget, Paperwork Reduction Project (0704-0188), Washington, DC 20503.

1. AGENCY USE ONLY *(Leave blank)*	2. REPORT DATE	3. REPORT TYPE AND DATES COVERED
	June 1994	Technical Memorandum

4. TITLE AND SUBTITLE

Theoretical, Experimental, and Computational Evaluation of a Tunnel Ladder Slow-Wave Structure

5. FUNDING NUMBERS

WU–235–01–1C

6. AUTHOR(S)

Thomas M. Wallett and A. Haq Qureshi

7. PERFORMING ORGANIZATION NAME(S) AND ADDRESS(ES)

National Aeronautics and Space Administration
Lewis Research Center
Cleveland, Ohio 44135–3191

8. PERFORMING ORGANIZATION REPORT NUMBER

E–8946

9. SPONSORING/MONITORING AGENCY NAME(S) AND ADDRESS(ES)

National Aeronautics and Space Administration
Washington, D.C. 20546–0001

10. SPONSORING/MONITORING AGENCY REPORT NUMBER

NASA TM–106642

11. SUPPLEMENTARY NOTES

Thomas M. Wallett, NASA Lewis Research Center, and A. Haq Qureshi, NASA Resident Research Associate at Lewis Research Center. Responsible person, Thomas M. Wallett, organization code 5620, (216) 433–3673.

12a. DISTRIBUTION/AVAILABILITY STATEMENT

Unclassified - Unlimited
Subject Category 33

12b. DISTRIBUTION CODE

13. ABSTRACT (*Maximum 200 words*)

The dispersion characteristics of a tunnel ladder circuit in a ridged wave guide were experimentally measured and determined by computer simulation using the electromagnetic code MAFIA. To qualitatively estimate interaction impedances, resonance frequency shifts due to a perturbing dielectric rod along the axis were also measured indicating the axial electric field strength. A theoretical modeling of the electric and magnetic fields in the tunnel area was also done.

14. SUBJECT TERMS

Tunnel ladder structure; Dispersion; Interaction impedance

15. NUMBER OF PAGES
19

16. PRICE CODE
A03

17. SECURITY CLASSIFICATION OF REPORT	18. SECURITY CLASSIFICATION OF THIS PAGE	19. SECURITY CLASSIFICATION OF ABSTRACT	20. LIMITATION OF ABSTRACT
Unclassified	Unclassified	Unclassified	